

## STUDIES ON THE DYNAMICS OF TWO BILATERALLY COUPLED PERIODIC GUNN OSCILLATORS USING MELNIKOV TECHNIQUE

Bishnu C. Sarkar<sup>1, \*</sup>, Manoj Dandapathak<sup>2</sup>, Suvra Sarkar<sup>3</sup>, and Tanmoy Banerjee<sup>1</sup>

<sup>1</sup>Physics Department, Burdwan University, Burdwan 713104, India

<sup>2</sup>Physics Department, Hooghly Mohsin College, Chinsurah, Hooghly 712101, India

<sup>3</sup>Electronics Department, Burdwan Raj College, Burdwan 713104, India

**Abstract**—Dynamical stability of a system of bilaterally coupled periodic Gunn oscillators (BCPGO) has been studied employing Melnikov's global perturbation technique. In the BCPGO system, a fractional part of the output signal of one oscillator is injected into the other through a coupling network. The injected signal is considered as a perturbation on the free running dynamics of the receiving oscillator and the amount of perturbation is quantified by a parameter named coupling factor (CF). The limiting values of CFs leading to chaotic dynamics of the BCPGO system are predicted analytically by calculating the Melnikov functions (MFs) in the respective cases. Also the effect of the frequency detuning (FD) between the Gunn Oscillators (GOs) on the computed values of MFs has been examined. A thorough numerical simulation of the BCPGO dynamics has been done by solving the system equations. The obtained results are in qualitative agreement with the analytically predicted observations regarding the roles of the system parameters like CF and FD.

### 1. INTRODUCTION

In past few decades, researchers have shown enormous interest in studying the dynamical behavior of different coupled nonlinear oscillators. This is mainly due to the huge application potential of

---

*Received 3 December 2012, Accepted 17 January 2013, Scheduled 24 January 2013*

\* Corresponding author: Bishnu Charan Sarkar (bcsarkar\_phy@yahoo.co.in).

coupled systems in various fields of science and engineering [1–4]. In the field of electronic communication, coupled oscillators play important roles in generating spectrally pure signals, combining power of signals from different sources, coherent modulation and detection process, chaos generation etc. [5–7]. Generally, coupled modes are either unilateral type (having master-slave configuration) [8] or bilateral type (i.e., the output of one is applied to the input of the other) [9]. Several interesting dynamical phenomena like synchronization, quasi-periodicity, intermittency and chaos are observed in coupled oscillators due to their inherent nonlinearity [7]. In [9] the phase-dynamics and synchronization of a system of two coupled Van der Pol oscillators under external harmonic force has been studied. [10] focuses on synchronization and bifurcation effects in periodically driven coupled non-identical Duffing oscillators. The mechanism of synthesizing a hyperchaotic oscillator by use of two coupled chaotic Colpitts oscillators is discussed in [11].

Recently, authors have reported some works on the dynamics of X-band microwave GOs [12–14]. In [12] generation of chaotic microwave oscillations in a driven under-biased GO was illustrated. The bilateral coupling between two such microwave chaotic GOs was thoroughly studied in [13]. In [14] the behavior of a system of BCPGO was studied experimentally and numerically. It showed that depending on the coupling strengths, the BCPGO system exhibits synchronized, quasi-periodic or chaotic states. However, considering the system-complexity, analytical predictions on the complete dynamics of BCPGO is a formidable task. To the knowledge of the authors, not much works have been reported in the literature on this problem. In the present paper, we explore this problem with the help of well-known Melnikov method of nonlinear analysis [15–17]. It is a global perturbation method and can be applied to any system that is perturbed by small damping and periodic forcing terms. Considering the internal damping of the GOs and coupled signal as small perturbations, we find the MF of the system. The knowledge of the MF would help us to predict the system response.

The paper is organized in the following way. In Section 2, using the circuit theoretic model of the GOs we have formulated mathematical equations of the BCPGO system. In Section 3, using the system equations, the expression of the MF for each oscillator is derived and the effects of variation of CFs as well as FD between two oscillators on the MF are calculated. It helps to predict the dynamics of each oscillator in the coupled system analytically. We present in Section 4, the results of numerical integration of system differential equations and compare them with the analytical predictions. Some concluding

discussions are given in Section 5.

## 2. MATHEMATICAL MODEL OF BCPGO SYSTEM

Figure 1 shows the functional block diagram of the BCPGO system, where  $i$ -th GO ( $i = 1, 2$ ) is coupled bi-directionally with the  $j$ -th GO ( $j = 2, 1$ ) through coupling networks characterized by CFs  $k_{ij}$  and  $k_{ji}$ , respectively.  $k_{ij}$  (or  $k_{ji}$ ) indicates the fraction of  $j$ -th ( $i$ -th) GO output applied as injected signal into  $i$ -th ( $j$ -th) GO in the coupled system. In isolated condition, both GOs are considered to operate in stable periodic mode but in general may have different free running frequencies and output amplitudes. In a GO, a Gunn diode is mounted inside a resonant cavity and shows negative differential resistance (NDR) property under suitable biasing condition. In the equivalent circuit of the oscillator [14], Gunn diode can be modeled by series combination of two nonlinear voltage sources ( $v_r$  and  $v_c$ ). Considering cubic type nonlinearity [14], we write  $v_r$  and  $v_c$  as:

$$v_r = -\beta_1 i + \beta_3 i^3 \tag{1}$$

$$v_c = -\alpha_1 q + \alpha_3 q^3 \tag{2}$$

Here  $i$  ( $= \frac{dq}{dt}$ ) and  $q$  are the instantaneous current and charge, respectively;  $\alpha_1, \alpha_3, \beta_1, \beta_3$  are the bias voltage dependent device parameters [14]. The resonant cavity of a GO is replaced by a series combination of inductor  $L$ , capacitor  $C$ , and resistor  $R$ . Here  $R$  includes the load resistance ( $R_L$ ) along with the lumped resistance of the cavity. Using this circuit theoretic model, the equivalent circuit of the BCPGO system is shown in Fig. 2.

Here, coupling of the  $j$ -th oscillator with the  $i$ -th oscillator is ensured by including an additional voltage source (proportional to the current in the latter one). Using Kirchoffs' mesh law in the equivalent

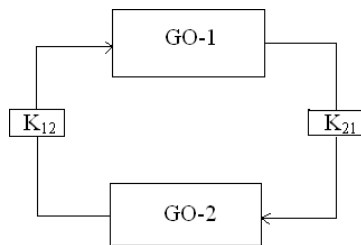


**Figure 1.** Simplified block diagram of bilaterally coupled Gunn oscillator system.

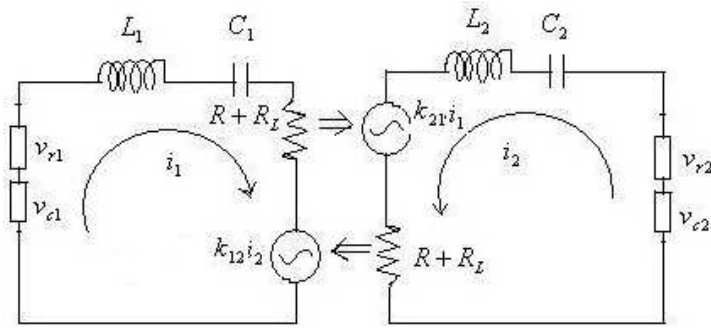


**Figure 2.** Equivalent circuit of BCPGO system.

circuit, system equations can be written in normalized form as,

$$\frac{d^2q_1}{d\tau^2} = a_1q_1 - b_1q_1^3 + c_1\frac{dq_1}{d\tau} - d_1\left(\frac{dq_1}{d\tau}\right)^3 + k_{12}\left(\frac{dq_2}{d\tau} - \frac{dq_1}{d\tau}\right) \quad (3)$$

$$\frac{d^2q_2}{d\tau^2} = a_2q_2 - b_2q_2^3 + c_2\frac{dq_2}{d\tau} - d_2\left(\frac{dq_2}{d\tau}\right)^3 + k_{21}\left(\frac{dq_1}{d\tau} - \frac{dq_2}{d\tau}\right) \quad (4)$$

Here we put  $a_i = \alpha_1 C_i - 1$ ,  $b_i = \alpha_3 C_i$ ,  $c_i = \frac{\beta_1 - R_i - R_{Li}}{\omega_{ri} L_i}$ ,  $d_i = \frac{\beta_3 \omega_{ri}}{L_i}$ . Physically,  $a_i$  and  $b_i$  indicate relative contributions of linear and cubic restoring forces. Similarly,  $c_i$  and  $d_i$  are the measures of linear and cubic damping forces. The normalized time  $\tau$  is  $\omega_{ri} t$  and  $\omega_{ri} = \frac{1}{\sqrt{L_i C_i}}$  represents the resonant frequency of the  $i$ -th cavity. To have identical time-scale for two GOs, we take passive parameters of the cavities so adjusted that  $\omega_{r1} = \omega_{r2}$ . However, due to natural difference in the DC biasing condition of the GOs, their oscillation frequencies may be different in general.

### 3. ANALYTICAL APPROACH USING MELNIKOV METHOD

The dynamical properties of the BCPGO system can be studied by solving the system Equations (3) and (4). But due to its high nonlinear character it is difficult to obtain a closed form solution of the system equations. Hence we propose to examine the system dynamics by applying Melnikov technique [15–17]. It requires the evaluation of Melnikov function (MF) of each oscillator that can be obtained from the total Hamiltonian ( $H$ ) of the system. For this purpose, we rewrite (3) and (4) as a set of four first-order coupled differential

equations as given in (5), by introducing two new state variables  $p_1$  and  $p_2$

$$\dot{q}_1 = p_1 \tag{5a}$$

$$\dot{p}_1 = a_1 q_1 - b_1 q_1^3 + c_1 p_1 - d_1 (p_1)^3 + k_{12} (p_2 - p_1) \tag{5b}$$

$$\dot{q}_2 = p_2 \tag{5c}$$

$$\dot{p}_2 = a_2 q_2 - b_2 q_2^3 + c_2 p_2 - d_2 (p_2)^3 + k_{21} (p_1 - p_2) \tag{5d}$$

The Hamiltonian ( $H$ ) of the coupled system is a function of the parameters  $q_i$  and  $p_i$  ( $i = 1, 2$ ) used in (5). The expression of  $H$  is a sum of unperturbed energies of the component systems, their self-perturbation energies due to internal damping and the perturbation energy due to bilateral coupling. Thus,

$$H = H_{01}(q_1, p_1) + H_{p1}(q_1, p_1) + H_{02}(q_2, p_2) + H_{p2}(q_2, p_2) \pm H_{pc}(q_1, p_1, q_2, p_2). \tag{6}$$

Here,  $H_{0i}(q_i, p_i)$  and  $H_{pi}$  represent, respectively, the unperturbed and the self-perturbed Hamiltonian respectively of  $i$ -th oscillator. Since parameters  $c$  and  $d$  are small in magnitude, the damping terms are considered as small perturbations.  $H_{pc}(q_i, q_j, p_i, p_j)$  is the perturbation term due to coupling between  $i$ -th and  $j$ -th GO. Their expressions are obtained as follows:

$$H_{0i}(q_i, p_i) = \frac{1}{2} p_i^2 + \frac{1}{2} q_i^2 + \frac{1}{4} q_i^4 \tag{7a}$$

$$H_{pi}(q_i, p_i) = -c_i q_i p_i + d_i q_i p_i^3 \tag{7b}$$

$$H_{pc}(q_i, q_j, p_i, p_j) = -k_{ij} (p_j - p_i) q_i - k_{ji} (p_i - p_j) q_j. \tag{7c}$$

To calculate MF for the  $i$ -th GO, we consider the  $j$ -th GO in a steady periodic condition. So, the state variables of the  $j$ -th GO,  $q_j$  and  $p_j$  are written as

$$q_j = A_{0j} \sin(\omega_{0j} \tau) \tag{8a}$$

$$p_j = A_{0j} \omega_{0j} \cos(\omega_{0j} \tau) \tag{8b}$$

The free running amplitude and the frequency of oscillation of the  $j$ -th GO would be obtained as [14],  $A_{0j}^2 = \frac{4c_j}{3d_j \omega_{0j}^2}$  and  $\omega_{0j}^2 = \frac{a_j}{2} [\sqrt{1 + \frac{4b_j c_j}{d_j a_j^2}} - 1]$ , respectively.

To get the state variables,  $q_i$  and  $p_i$ , of the  $i$ -th GO, its unperturbed Hamiltonian,  $H_{0i}(q_i, p_i)$  as given in 7(a), is equated to zero. Solving the relation, we obtain,

$$q_i = \sqrt{\frac{2a_i}{b_i}} \operatorname{sech}(\sqrt{a_i}\tau) \quad (9a)$$

$$p_i = -\sqrt{\frac{2}{b_i}} a_i \operatorname{sech}(\sqrt{a_i}\tau) \tanh(\sqrt{a_i}\tau) \quad (9b)$$

This indicates that the trajectory of  $i$ -th GO in the state space is a homoclinic orbit. The MF of  $i$ -th GO is derived as [16],

$$M_i(\tau_0) = \int_{-\infty}^{\infty} \{H_{0i}, (H_{pi} + H_{pc})\} d\tau \quad (10)$$

where

$$\{H_{0i}, (H_{pi} + H_{pc})\} = \frac{\partial H_{0i}}{\partial q_i} \frac{\partial (H_{pi} + H_{pc})}{\partial p_i} - \frac{\partial H_{0i}}{\partial p_i} \frac{\partial (H_{pi} + H_{pc})}{\partial q_i} \quad (11)$$

Using Equations (7) to (11), and simplifying one gets,

$$\begin{aligned} M_i(\tau_0) &= \frac{8 a_i^{3/2} c_i}{3 b_i} - \frac{48 a_i^{7/2} d_i}{35 b_i^2} - \frac{8 k_{ij} a_i^{3/2}}{3 b_i} \\ &+ \frac{k_{ji} A_{0j} \pi \sqrt{2a_i} \operatorname{sech}(\pi\omega_{0j}/2\sqrt{a_i})}{b_i^{1/2}} \sin(\omega_{0j}\tau_0) \\ &- \frac{\pi\omega_{0j} k_{ji}}{3b_i} (4a_i + \omega_{0j}^2) \operatorname{sech}(\pi\omega_{0j}/4\sqrt{a_i}) \operatorname{cosech}(\pi\omega_{0j}/4\sqrt{a_i}) \sin(\omega_{0j}\tau_0) \\ &\mp \sqrt{2\pi} A_{0j} \omega_{0j}^2 \frac{k_{ij}}{b_i a_i^{3/2}} \operatorname{sech}(\pi\omega_{0j}/2\sqrt{a_i}) \sin(\omega_{0j}\tau_0) \end{aligned} \quad (12)$$

Here  $\tau_0$  indicates the time of occurrence of the first homoclinic intersection between stable and unstable orbits. The evaluation of  $M_i(\tau_0)$  for different values of the system design parameters can predict the dynamics of  $i$ -th GO in the BCPGO system. The MF gives the distance between stable and unstable manifolds. If, for a given set of parameters, the sign of the MF changes from negative to positive, it is predicted that the system would exhibit chaotic behavior at that condition. Critical values of system parameters required for the transition from a stable to a chaotic mode can be obtained from zero value of MF. In the present work, we study the effect of CFs and the FDs between two GOs on the system behavior by evaluating the MF.

### 3.1. Computed Variation of MF with CFs

In order to analytically predict the system-response, we compute  $M_i(\tau_0)$  for some chosen values of GO-parameters and CFs. Take, for example,  $\omega_{01}$  and  $\omega_{02}$  as 1.29 and 1.16, with  $A_{01}$  and  $A_{02}$  as 2.83 and 2.43, respectively. This is done by suitably adjusting parameters  $a, b, c$  and  $d$ . In this condition,  $M_i(\tau_0)$  is evaluated for different values of  $k_{ij}$  and  $k_{ji}$ . We take the value of  $\sin(\omega_{0j}\tau_0)$  as 1 (its maximum value) without any loss of generality (since  $\tau_0$  is arbitrary). The obtained variation of  $M_i(\tau_0)$  is shown in Fig. 3 where  $k_{ij}$  and  $k_{ji}$  are plotted along the lower and upper horizontal directions, respectively. The change of sign of  $M_i(\tau_0)$  from negative to positive is observed at some critical values of  $k_{ij}$  and the magnitudes of these values increase for increasing  $k_{ji}$ . This means that  $i$ -th GO would undergo a transition from a stable state to a chaotic state due to the injected signal of specific amount from  $j$ -th GO. Also the variation of  $M_i(\tau_0)$  with  $k_{ji}$  at fixed values of  $k_{ij}$  indicates a transition of  $i$ -th GO from a chaotic state to a stable state because of the variation of the amount of signal taken from it. In brief, the dynamics of a GO in the BCPGO system not only depends on the amount of signal injected into it, but also on the amount of signal taken from it.

To study the effect of variation of a particular CF on the system-dynamics, variations of  $M_i(\tau_0)$  and  $M_j(\tau_0)$  with  $k_{ij}$  (for a fixed value of  $k_{ji} = 0.2$ ) are calculated and simultaneously plotted in Fig. 4. It is observed that as  $k_{ij}$  increases,  $i$ -th GO transits from a stable state to

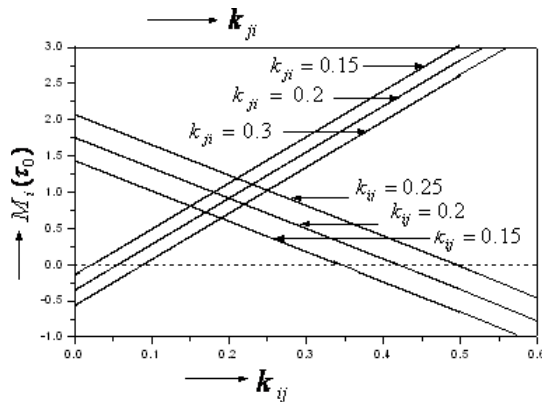


**Figure 3.** Variation of the Melnikov function of the  $i$ -th GO with  $k_{ij}$  (lower  $x$ -axis), and  $k_{ji}$  (upper  $x$ -axis), other parameters are ( $A_{0i} = 2.83$ ,  $\omega_{0i} = 1.29$ ,  $A_{0j} = 2.43$ ,  $\omega_{0j} = 1.16$ ).

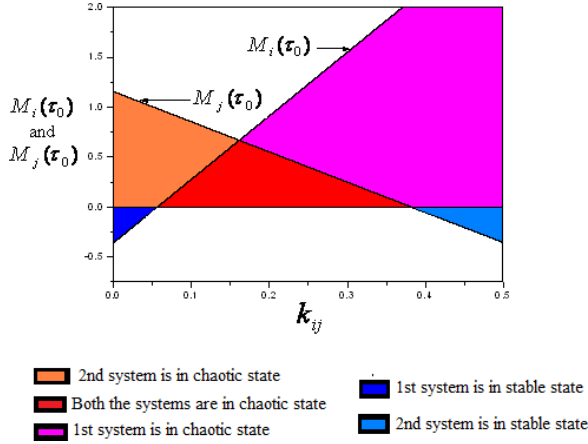


**Figure 4.** Variation of the Melnikov function for both the GOs in the BCPGO system with  $k_{ij}$ , (other parameters are  $k_{ji} = 0.2$ ,  $A_{0i} = 2.83$ ,  $\omega_{0i} = 1.29$ ,  $A_{0j} = 2.43$ ,  $\omega_{0j} = 1.16$ ).

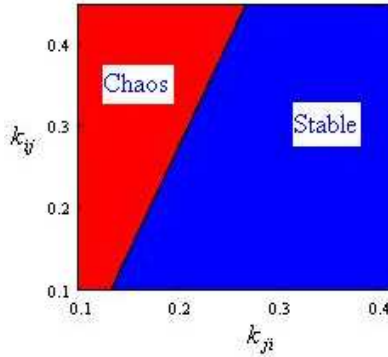


**Figure 5.** Analytically predicted  $k_{ij}$ - $k_{ji}$  parameter space plot indicating stable oscillatory (Blue colour) and unstable chaotic (Red color) mode of operation of the  $i$ -th GO for  $A_{0i} = 2.83$ ,  $\omega_{0i} = 1.29$ ,  $A_{0j} = 2.43$ ,  $\omega_{0j} = 1.16$ .

a chaotic one and the  $j$ -th GO transits from a chaotic state to a stable one. However, for a range of  $k_{ij}$  ( $0.06 < k_{ij} < 0.38$ ), both GOs are in chaotic mode. When  $k_{ij} > 0.38$ , the MF of  $i$ -th GO remains positive but that of  $j$ -th GO changes to negative value after crossing zero. Therefore, in this condition although  $i$ -th GO is in a chaotic mode,  $j$ -th GO changes to a periodic state. The computations with different



values of  $k_{ji}$ , give similar characteristics of the system response as described above. However, the critical values needed for transition from one state to the other and range of parameter  $k_{ij}$  where both GOs are in chaotic state, are different.

In Fig. 5, the predicted dynamical states of  $i$ -th GO in the BCPGO system have been shown for different pairs of CFs. With the values of GO parameters taken as above, the magnitude and the sign of the MF computed using (12) are used to predict the state of the GO. The results given in the parameter space  $k_{ij}$ - $k_{ji}$  show that, with the GO parameters under consideration,  $i$ -th GO is in chaotic state for all reasonable values of injected signal. But if the injected signal into  $j$ -th GO taken from  $i$ -th GO increases, the chaotic state of  $i$ -th GO changes to a stable state. Also, the more would be the amount of signal injected into  $i$ -th GO, the greater would be the required amount of signal to be injected into  $j$ -th GO for quenching the chaotic state of  $i$ -th GO.

### 3.2. Computed Variations of MF Values with the FD between GOs

To examine the effect of relative frequencies of the GOs on the system response, the MF of a particular GO is calculated with a suitable FD between the oscillators in the system. With a fixed set of  $k_{ij}$  and  $k_{ji}$ , the variation of  $M_i(\tau_0)$  is observed with the variation of  $(\omega_{0j})$ . Fig. 6 represents computed results obtained for fixed values of  $\omega_{0i}$ ,  $k_{ji}$  and oscillator output amplitudes (as shown in the caption of Fig. 6). With a moderate strength of the injected signal to the  $i$ -th GO ( $k_{ij} = 0.25$ )

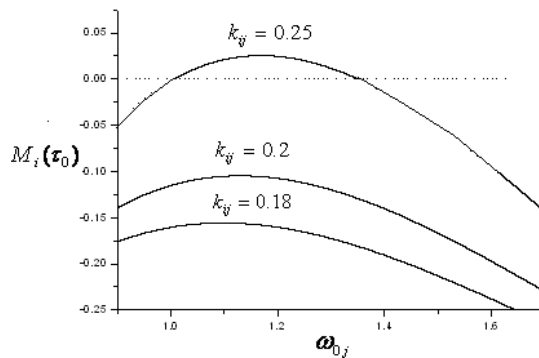


**Figure 6.** Variation of the Melnikov function of the  $i$ -th GO with free running frequency of the  $j$ -th GO for  $k_{ji} = 0.2$ ,  $A_{0i} = 2.83$ ,  $\omega_{0i} = 1.29$ ,  $A_{0j} = 1.65$ ,  $\omega_{0j} = 1.18$ .

the variation of  $\omega_{0i}$  around  $\omega_{0j}$  would cause chaotic transition of its dynamics. This is evident from the change of sign of the MF from negative to positive value. However, the possibility of transition to chaotic oscillations has sensitive dependence on the amplitudes of the GOs and CFs. Even though a quantitative prediction of the system dynamics from the derivation of MF is difficult to get, a qualitative prediction is possible using a sufficient number of computed results.

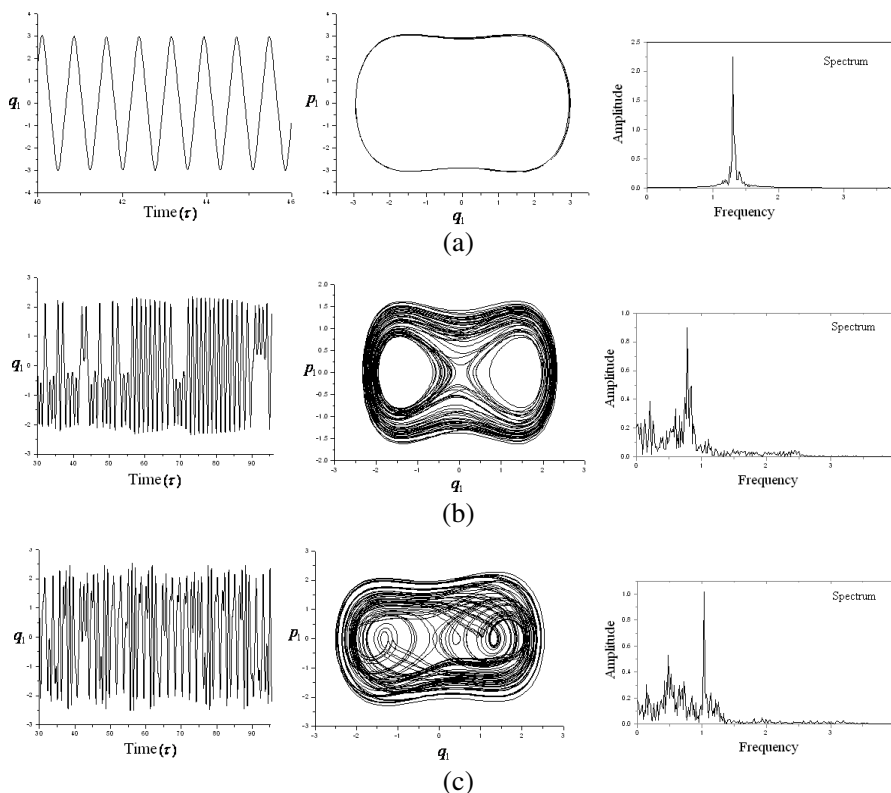


**Figure 7.** Time domain plot, state space trajectory and frequency spectrum of the  $i$ -th GO for (a)  $k_{ij} = 0.02$ , (b)  $k_{ij} = 0.081$ , and (c)  $k_{ij} = 0.39$  (Other parameters are  $k_{ji} = 0.2$ ,  $A_{0i} = 2.83$ ,  $\omega_{0i} = 1.29$ ,  $A_{0j} = 2.43$ ,  $\omega_{0j} = 1.16$ ).

#### 4. NUMERICAL ANALYSIS

To obtain real-time dynamics of GOs in the BCPGO system, Equations (3) and (4) are solved numerically. For this purpose, 4th order Runge-Kutta numerical integration technique is applied. In the simulation, the step size for time increment is taken as 0.001. To get a steady state response, a sufficient number of initial results are discarded to avoid transients. From the simulated results time development of the output of each GO ( $q_i$  and  $q_j$ ), their state space trajectories (in  $q_i - p_i$  and  $q_j - p_j$  planes) and the frequency spectra of the time series data are obtained under different conditions of operation. Fig. 7 and Fig. 8 depict a few results for  $i$ -th and  $j$ -th GOs respectively for some fixed values of CFs.

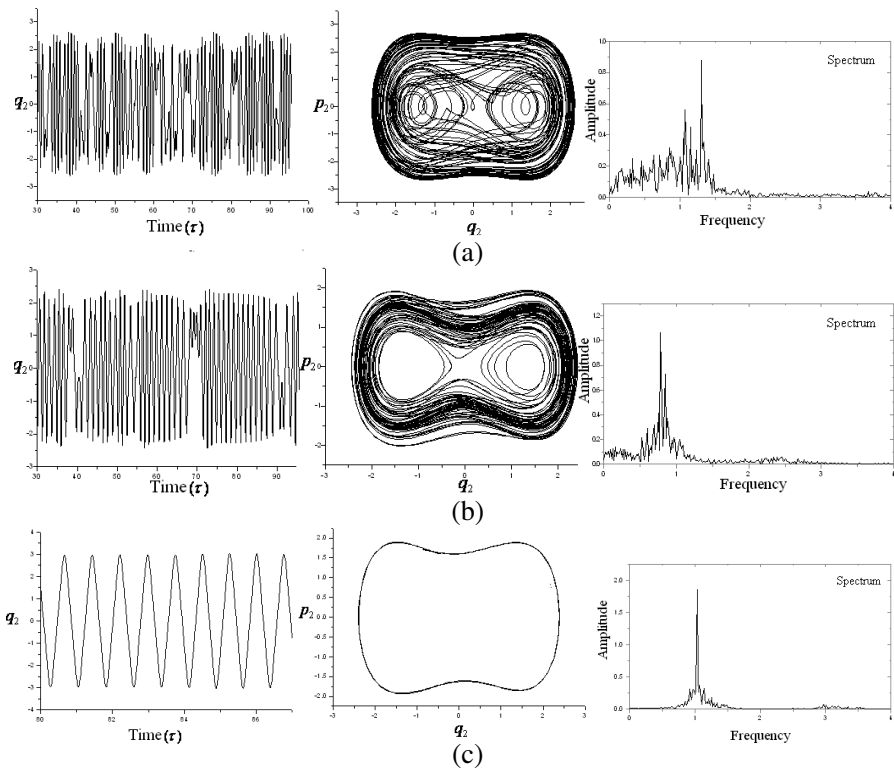


**Figure 8.** Time domain plot, state space trajectory and frequency spectrum of the  $j$ -th GO for (a)  $k_{ij} = 0.02$ , (b)  $k_{ij} = 0.081$ , and (c)  $k_{ij} = 0.39$  (Other parameters are  $k_{ji} = 0.2$ ,  $A_{0i} = 2.83$ ,  $\omega_{0i} = 1.29$ ,  $A_{0j} = 2.43$ ,  $\omega_{0j} = 1.16$ ).

The effects of variation of the frequency of  $j$ -th GO on the dynamics of  $i$ -th GO is studied numerically keeping the strength of the coupling coefficients fixed. The obtained results are presented in Fig. 9. It shows that, in an isolated condition both the GOs are considered to operate in stable periodic mode with different free running frequencies ( $\omega_{0i} = 1.29$  and  $\omega_{0j} = 1.16$ ) and output amplitudes ( $A_{0i} = 2.83$  and  $A_{0j} = 2.43$ ). As they are bilaterally coupled, the combined dynamics is found to depend on the strengths of the CFs and FDs between them. Fig. 7 and Fig. 8 give numerically obtained responses of  $i$ -th and  $j$ -th GO, respectively. The fixed parameters of the system leading to these responses are given in the captions of the figures. With a fixed moderate value of  $k_{ji}$  ( $= 0.2$ ), the parts (a), (b) and (c) of Fig. 7 and Fig. 8 show the responses with small (0.02), comparable

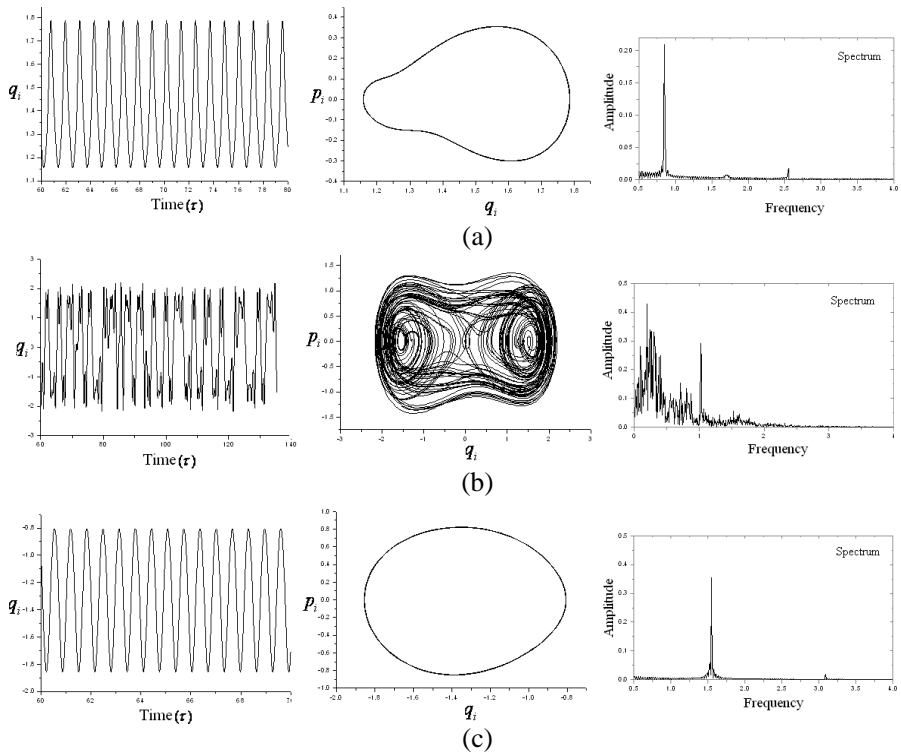


**Figure 9.** Time domain plot, state space trajectory and frequency spectrum of the  $i$ -th GO for (a)  $\omega_{0j} = 0.97$ , (b)  $\omega_{0j} = 1.18$ , and (c)  $\omega_{0j} = 1.78$  (Other parameters are  $k_{ij} = 0.25$ ,  $k_{ji} = 0.2$ ,  $A_{0i} = 2.83$ ,  $\omega_{0i} = 1.29$ ,  $A_{0j} = 1.65$ ).

(0.081) and large (0.39) values of  $k_{ij}$ , respectively. For the CF-set given in part (a) of the figures,  $i$ -th and  $j$ -th GOs are periodic and chaotic respectively as is evident from the real-time, phase-plane and frequency-spectrum of the oscillator outputs. When both CFs are of moderate and comparable value, the GOs show chaotic oscillations (part (b) of the figures.)

In the case shown in part (c) of the figures the roles of  $i$ -th and  $j$ -th GOs are reversed, i.e.,  $i$ -th GO becomes chaotic and  $j$ -th GO becomes periodic. This is natural in a bilaterally coupled system where the relative values of  $k_{ij}$  and  $k_{ji}$  are interchanged as given in part (a). For the confirmation of the chaotic state, the time series data of  $i$ -th ( $j$ -th) GO, the time-series data  $q_i$  ( $q_j$ ) as obtained from the numerical simulation is analyzed using the CDA software [18] and the estimation of the maximum Lyapunov exponent (MLE) is done. The positive value of MLE confirms the chaotic state of the concerned oscillation. For the set used in part (a) only the MLE for  $q_j$  is positive (0.047). For that used in part (b) the MLEs for  $q_i$  and  $q_j$  are both positive (0.027 and 0.032, respectively) and for the set used in part (c) only the MLE of  $q_i$  is positive (0.047). Hence the conclusions regarding the chaotic states of the GOs are consistent with the obtained values of MLEs. These observations are in good agreement with the analytical predictions given in previous section (Fig. 4).

Figure 9 shows for a fixed set of values of CFs, the output of  $i$ -

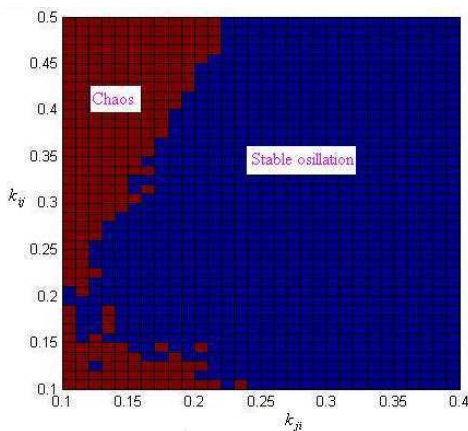


**Figure 10.**  $k_{ij}$ - $k_{ji}$  parameter space plot of  $i$ -th GO (as obtained from the simulated results) indicating stable oscillatory (Blue colour) and unstable chaotic (Red color) mode of operation for  $A_{0i} = 2.83$ ,  $\omega_{0i} = 1.29$ ,  $A_{0j} = 2.43$ ,  $\omega_{0j} = 1.16$ .

th GO becomes in chaotic mode within a specific range of  $\omega_{0j}$ . Both above and below this range, it oscillates in a periodic condition. These results follow the predictions as obtained from the variation of the MF of  $i$ -th GO with  $\omega_{0j}$  (Fig. 6). The role of two CFs ( $k_{ij}$  and  $k_{ji}$ ) on the dynamical behavior of the GOs (stable periodic or unstable chaotic) in the coupled system is examined using simulated results and is plotted in the  $k_{ij}$ - $k_{ji}$  parameter space as shown in Fig. 10. From this figure it is observed, for a given value of  $k_{ji}$ , there is a transition in the oscillator behavior from stable periodic mode to chaotic mode as  $k_{ij}$  increases. This observation is in good agreement with the analytically predicted results given in Fig. 5.

## 5. CONCLUSION

The dynamics of a system of two GOs, coupled bilaterally, has been examined analytically and numerically. The analytical method, based on Melnikov technique, considers the injected signal due to coupling as a perturbation term. The amount of perturbation is quantified by the CFs ( $k_{ij}$  and  $k_{ji}$ ). The validity of the method rests on the choice of CFs within a moderate range as it is a perturbation technique. The analytical predictions on the system response have been done by finding the MF of a GO for different values of CFs and FDs. The amount of signal injected into as well as that taken from an oscillator, have vital role in the system dynamics. This is evident from the effects of both  $k_{ij}$  and  $k_{ji}$  on the dynamics of the  $i$ -th oscillator. Moreover, the behavior of one oscillator is modified by the variation of frequency of the other. For a given set of CFs, it is possible to make one oscillator chaotic for a range of frequencies of the other. As expected intuitively, the transition to an unstable state (chaotic) is found to occur when the FD between the oscillators is moderate for reasonable values of the CFs. For small values of FD, a state of synchronization may occur and for a large FD, the interaction between oscillators is not appreciable. The numerical integration of the system equation provides results which qualitatively agree with the analytical predictions. The information regarding the overall dynamics of a BCPGO system reported in the paper would be useful for the design of chaotic oscillators at microwave frequencies.

## ACKNOWLEDGMENT

Authors (BCS, SS, TB) thankfully acknowledge partial financial support from the BRNS, DAE, Government of India through sponsored Research Project.

## REFERENCES

1. Kuramoto, Y., *Chemical Oscillations, Waves and Turbulence*, Springer, Berlin, 1984.
2. Boi, S., I. D. Couzin, N. D. Buono, N. R. Franks, and N. F. Britton, "Coupled oscillators and activity waves in ant colonies," *Proceedings Royal Society*, 371–378, 1998.
3. Mulet, J., C. Mirasso, T. Heil, and I. Fischer, "Synchronization scenario of two distant mutually coupled semiconductor lasers," *Journal of Optics B: Quantum and Semi Classical Optics*, Vol. 6, 97–105, 2004.
4. Ram, R. J., R. Sporer, H. R. Blank, and R. A. York, "Chaotic dynamics in coupled microwave oscillators," *IEEE Trans. Microwave Theory and Technique*, Vol. 48, 1909–1916, 2000.
5. Crawford, J. A., *Advanced Phase Lock Technique*, Artech House, Inc., 2008.
6. Liao, P. and R. A. York, "A new phase-shifterless beam scanning technique using arrays of coupled oscillators," *IEEE Trans. Microwave Theory and Technique*, Vol. 41, 1810–1815, 1993.
7. Hilborn, R. C., *Chaos and Nonlinear Dynamics*, Oxford University Press, 2000.
8. Kurokawa, K., "Injection locking of microwave solid state oscillator," *Proceedings of IEEE*, Vol. 61, 1386–1410, 1973.
9. Anishchenko, V., S. Astakhov, and T. Vadivasova, "Phase dynamics of two coupled oscillators under external periodic force," *Europhysics Letters*, Vol. 86, 2009.
10. Vincent, U. E. and A. Kenfack, "Synchronization and bifurcation structures in coupled periodically forced non-identical duffing oscillators," *Physica Scripta*, Vol. 77, 1–7, 2008.
11. Cenys, A., A. Tamasevicius, A. Baziliauskus, R. Krivickas, and E. Lindberg, "Hyperchaos in coupled Colpitts oscillators," *Chaos, Solitons and Fractals*, Vol. 17, 349–353, 2003.
12. Sarkar, B. C., C. Koley, A. K. Guin, and S. Sarkar, "Some numerical and experimental observations on the growth of oscillations in an X-band Gunn oscillator," *Progress In Electromagnetics Research B*, Vol. 40, 325–341, 2012.
13. Sarkar, B. C., C. Koley, A. K. Guin, and S. Sarkar, "Studies on the dynamics of a system of bilaterally coupled chaotic Gunn oscillators," *Progress In Electromagnetics Research B*, Vol. 42, 93–113, 2012.

14. Sarkar, B. C., D. Sarkar, S. Sarkar, and J. Chakraborty, "Studies on the dynamics of bilaterally coupled X-band Gunn oscillators," *Progress In Electromagnetics Research B*, Vol. 32, 149–167, 2011.
15. Holmes, J. P. and J. E. Marsden, "Melnikovs method and Arnold diffusion for perturbation of integrable Hamiltonian systems," *Journal of Math. Physics*, Vol. 23, No. 4, 669–675, 1982.
16. Jordan, D. W. and P. Smith, *Nonlinear Ordinary Differential Equations: An Introduction for Scientists and Engineers*, 4th Edition, Oxford University Press, New York, 2007.
17. Chacon, R., "Melnikov method approach to control of Homoclinic/Heteroclinic chaos by weak harmonic excitations," *Phil. Trans. R. Soc. A*, Vol. 364, 2335–2351, 2006.
18. Sprott, J. C., *Chaos Data Analyser Package*, Web Address: [sprott.physics.wise.edu/cda.htm](http://sprott.physics.wise.edu/cda.htm).